Induction of Lysosomal Dilatation, Arrested Autophagy, and Cell Death by Chloroquine in Cultured ARPE-19 Cells

Young Hee Yoon,[1,2] *Kyung Sook Cho,*[2,3] *Jung Jin Hwang,*[4] *Sook-Jeong Lee,*[3] *Jeong A. Choi,*[3] *and Jae-Young Koh*[3]

Purpose. To characterize and investigate the mechanism of chloroquine (CQ) retinotoxicity in human retinal pigment epithelium–derived ARPE-19 cells.

Methods. Cultured ARPE-19 cells were exposed to 10 to 250 μM CQ, and cell death was quantified using a lactate dehydrogenase release assay. Autophagy was studied in ARPE-19 cells transfected with GFP-LC3. Lysosomes in living cells were stained and observed by live-cell confocal microscopy.

Results. After exposure to CQ, ARPE-19 cells developed cytosolic vacuoles within 1 hour and underwent cell lysis within 24 hours. The levels of LC3-II, beclin-1 and, p62, as well as the number GFP-LC3– and RPF-LC3–positive autophagic vacuoles (AVs), increased after CQ treatment, indicating that autophagy was activated. However, lysosomal staining revealed that almost all AVs were separate from lysosomes; thus, fusion between AVs and lysosomes was completely blocked. In addition, the levels of ubiquitinated proteins and GFP-mHttp aggregates in ARPE-19 cells were increased by CQ, providing further evidence that autophagic degradation was inhibited.

Conclusions. CQ induces vacuole formation and cell death in ARPE-19 cells. Initially, vacuoles developed from enlarged lysosomes, followed by the activation of upstream steps in the autophagy pathway and the formation of LC3-positive AVs. Because CQ blocked the fusion of AVs with lysosomes, autophagic protein degradation was inhibited, indicating that CQ-induced retinotoxicity may be caused by the accumulation of potentially toxic ubiquitinated proteins. (*Invest Ophthalmol Vis Sci.* 2010;51:6030–6037) DOI:10.1167/iovs.10-5278

Chloroquine (CQ), a 4-aminoquinoline compound, is a widely used antimalarial and anti-inflammatory agent.[1–3] The mechanism of action underlying the therapeutic efficacy of CQ is not completely known, but some biological effects of CQ may involve the inhibition of lysosomal functions.[4] Although CQ is a relatively safe drug with good efficacy under the conditions used clinically, certain side effects raise potential concerns. Of these, well-documented ocular side effects involving the retina are probably the most serious.[5,6] Previous studies have demonstrated that CQ can cause retinal cell damage in vitro and in vivo.[7–9] The retinal cellular component that seems to be the primary target of CQ toxicity is the retinal pigment epithelium (RPE).[10,11]

The RPE is a single layer of cells adjacent to the photoreceptor outer segment (POS) of the retina. Given this location, the RPE plays critical roles in the maintenance of the POS, in part by removing shed rod and cone debris[12]; once endocytosed by endosome formation, this debris is ultimately degraded in lysosomes.[13] It has been proposed that abnormalities in lysosome-dependent degradation of shed POS debris can contribute to the degeneration of RPE cells. Accordingly, the retinotoxicity of CQ has been attributed to its inhibitory effect on lysosomal activity.[9] Because lysosomes are also a key element in autophagy, it is possible that CQ affects autophagy.

Autophagy or macroautophagy is activated under various cellular stress conditions such as starvation and oxidative stress. It is the only intracellular pathway for bulk degradation and recycling of long-lived proteins and cytoplasmic organelles such as mitochondria and endoplasmic reticulum (ER) and, thus, is essential for cellular viability.[14,15]

In the present study, we examined the characteristics and possible mechanisms of CQ-induced cytotoxicity in human RPE-derived ARPE-19 cells, focusing on the autophagic pathway.

Materials and Methods

Cell Culture

ARPE-19 cells were obtained from the American Type Culture Collection (CRL-2302; Manassas, VA) and were cultured in medium (Dulbecco's Modified Eagle Medium Nutrient Mixture F-12; Invitrogen, Carlsbad, CA) supplemented with 10% fetal bovine serum (FBS; Invitrogen) and penicillin-streptomycin (100 IU/mL-100 μg/mL; Lonza, Allendale, NJ) at 37°C in a humidified 5% CO_2 incubator. Cells were used after they reached approximately 80% confluence.

Drugs and Chemicals

CQ, MG132, antioxidant (Trolox; Hoffman-LaRoche, Basel, Switzerland), and rapamycin were purchased from Sigma (St. Louis, MO). The pan-caspase inhibitor z-VAD-FMK and N-acetyl-L-cysteine (NAC) were purchased from Calbiochem (San Diego, CA). Staurosporine was purchased from Alexis Biochemicals (Plymouth Meeting, PA). H_2O_2 was purchased from Merck (Darmstadt, Germany).

From the [1]Department of Ophthalmology, the [3]NRL Neural Injury Research Center and Department of Neurology, and the [4]Institute for Innovative Cancer Research, Asan Medical Center, University of Ulsan, College of Medicine, Seoul, Korea.

[2]These authors contributed equally to the work presented here and should therefore be regarded as equivalent authors.

Supported by the Korea Health Care Technology R&D Project, Ministry of Health, Welfare & Family Affairs, Republic of Korea (Grant A084270).

Submitted for publication January 27, 2010; revised May 14, 2010; accepted June 8, 2010.

Disclosure: **Y.H. Yoon**, None; **K.S. Cho**, None; **J.J. Hwang**, None; **S.-J. Lee**, None; **J.A. Choi**, None; **J.-Y. Koh**, None

Corresponding author: Jae-Young Koh, Department of Neurology & NRL Neural Injury Research Center, University of Ulsan College of Medicine, 388-1 Poongnap-Dong, Songpa-Gu, Seoul, Korea; jkko@amc.seoul.kr.

Investigative Ophthalmology & Visual Science, November 2010, Vol. 51, No. 11

Assessment of Cell Death

CQ-induced cell death was quantified by measuring lactate dehydrogenase (LDH) activity released into the culture medium.[16] LDH activity was estimated using an automated microplate reader (UVmax; Molecular Devices, San Francisco, CA) by measuring the rate of decrease in absorbance at 340 nm. After subtraction of background (sham-washed control cultures), LDH values were normalized to the mean maximal value (defined as 100%) in parallel cultures exposed to 1 mM H_2O_2 for 24 hours, conditions that caused complete cell death.

Caspase-3 Activity

Caspase-3 activity was measured with an assay kit (Caspase-3 Fluorescent Assay Kit; Peptron, Tae-Jeon, Korea) according to the manufacturer's protocol.

Measurement of Reactive Oxygen Species

The levels of intracellular reactive oxygen species (ROS) were measured using the fluorescent probe 5-(and-6)-carboxy-2′, 7′-dichlorohydrofluorescein diacetate (H_2-DCFDA) as described by the manufacturer (Molecular Probes, Eugene, OR). In brief, cells were incubated with 10 μM H_2-DCFDA for 15 minutes at 37°C and then washed in serum-free minimum essential medium (MEM; Invitrogen) without phenol red. Cells were observed under a fluorescence microscope and photographed.

Plasmids

The GFP-LC3 plasmid was constructed as follows: plasmid DNA containing the coding region of mouse microtubule-associated protein 1 light chain 3 (LC3; GenBank accession no. NM_026160) inserted into *Sal*I and *Not*I sites in the pSPORT1 vector was purchased from the Korea Research Institute of Bioscience and Biotechnology (Daejon, Korea). The LC3 coding region from the purchased construct was digested with *Sal*I and *Bam*HI (Promega, Madison, WI) and subcloned into the corresponding sites of the pAcGFP1-C1 vector (Clontech, Mountain View, CA). The completed GFP-LC3 plasmid was verified by DNA sequencing. The GFP-LC3 construct was transfected into cells using reagent (Lipofectamine 2000; Invitrogen), and its cellular expression was confirmed by Western blot analysis. The RFP-LC3 expression plasmid was a generous gift from Maria Colombo and Michel Rabinovitch (Universidad Nacional de Cuyo, Mendoza, Argentina).

Live-Cell Confocal Microscopy

For live-cell imaging experiments, ARPE-19 cells were stained with 75 nM solution in dimethyl sulfoxide (LysoTracker Green DND-26; Invitrogen) in MEM for 5 to 30 minutes in a humidified CO_2 incubator, transferred to Hanks' balanced salt solution (HBSS; Lonza), and observed under a confocal microscope at an excitation wavelength of 488 nm. Live-cell confocal images were obtained using a confocal imaging system (UltraView; PerkinElmer, Waltham, MA) attached to a transmission electron microscope (Eclipse TE2000; Nikon, Melville, NY). All fluorescence intensities are expressed in arbitrary units.

Immunocytochemistry

Cells were fixed in 4% paraformaldehyde for 1 hour at room temperature and were permeabilized with 0.2% Triton X-100 containing 1% bovine serum albumin (BSA) in phosphate-buffered saline (PBS) for 15 minutes. After blocking with 1% BSA, fixed cells were incubated overnight at 4°C with primary antibodies against ubiquitin (1:100 dilution; Dako, Carpinteria, CA) or lysosomal-associated membrane protein-1 (LAMP-1, 1:200 dilution; Hybridoma Bank, Iowa City, IA). The stained cells were washed and incubated for 2 hours at room temperature with AlexaFluor-conjugated secondary antibodies (AlexaFluor 555-donkey anti–mouse IgG 1:500 dilution or AlexaFluor 488-donkey anti–rabbit IgG 1:500 dilution; Molecular Probes, Leiden, The Netherlands). After incubation with secondary antibodies, cells were stained with the nuclear dye Hoechst 33342 (Invitrogen) in PBS for 2 minutes at room temperature. For negative controls, cultured cells were incubated with secondary antibody only.

Immunoblot Analysis

After washing with serum-free medium, cells were suspended in lysis buffer (20 mM Tris-Cl, pH 7.4, 150 mM NaCl, 1 mM EDTA, 1 mM EGTA, 1% Triton X-100, 2.5 mM sodium pyrophosphate, 1 μM Na_3VO_4, 1 μg/mL leupeptin, 1 mM phenylmethylsulfonyl fluoride) and centrifuged. Equal amounts of proteins were separated by SDS-PAGE on 10% or 12% polyacrylamide gels and transferred to polyvinylidene difluoride membranes (Millipore, Bedford, MA). The membranes were blocked with 3% nonfat dried milk for 1 hour and incubated overnight at 4°C with anti–LC3 (1:1000 dilution; Novus, Littleton, CO), anti–beclin-1, anti–cleaved caspase-3 (1:1000 dilution; Cell Signaling, Boston, MA), anti–β-actin (1:2000 dilution; Sigma), or anti–ubiquitin (1:1000 dilution; Dako) antibodies, followed by incubation with horseradish peroxidase-conjugated goat anti–rabbit IgG (1:10,000 dilution; Pierce, Woodstock, IL). For p62 immunoblotting, treatment with anti–p62 (1:500; Santa Cruz Biotech, Santa Cruz, CA) antibody was followed by treatment with horseradish peroxidase-conjugated goat anti–mouse IgG (1:10,000 dilution; Pierce). Immunoreactive proteins were visualized using a chemiluminescence substrate (Millipore) and quantitatively analyzed by densitometry using ImageJ software (developed by Wayne Rasband, National Institutes of Health, Bethesda, MD; available at http://rsb.info.nih.gov/ij/index.html). All experiments were performed at least in triplicate.

Statistical Analysis

All data are presented as mean ± SD. Student's *t*-tests were used to analyze differences between two groups. Multiple sets of data were

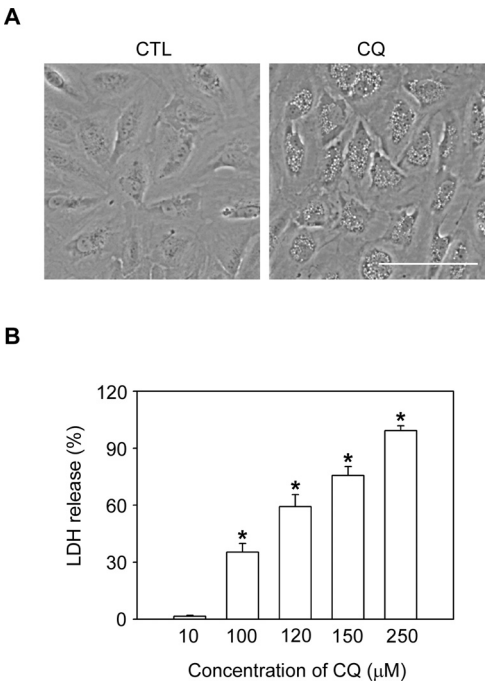

FIGURE 1. CQ induces vacuole formation and cell death. (**A**) Phase-contrast photomicrographs of sham-washed ARPE-19 cells (CTL, *left*) and cells 3 hours after the addition of 120 μM CQ (*right*). Note vacuolar changes in CQ-treated cells. Scale bar, 100 μm. (**B**) Measurements of LDH release into the medium of ARPE-19 cells after 24-hour exposure to the indicated concentrations of CQ, expressed as mean ± SD (*$P < 0.05$ compared with sham-washed controls; $n = 3$). After subtracting the sham-washed control background value, LDH concentrations were normalized to the mean maximal value in parallel cultures exposed for 24 hours to 250 μM CQ, which caused the death of all cells.

compared using one-way ANOVA followed by Fisher least significant difference post hoc tests. $P < 0.05$ was considered statistically significant.

Results

CQ-Induced Vacuole Formation and Cell Death

ARPE cells began to develop conspicuous vacuoles in their cytoplasm within 1 hour of exposure to 120 μM CQ (Fig. 1A) and proceeded to cell death within 24 hours. To determine the concentration dependence of CQ cytotoxicity, cells were exposed to 10 to 250 μM CQ for 24 hours, and LDH released into the medium was measured to quantify cell death. CQ caused virtually no cell death at 10 μM but was nearly 100% cytotoxic at 250 μM (Fig. 1B). The estimated LD_{50} was between 100 and 120 μM.

Increase of Autophagic Markers in CQ-Treated Cells

Compounds that inhibit lysosomal functions, such as CQ, are known to activate the autophagy cascade that is upstream of lysosomes. To measure autophagy after CQ treatment, we transfected ARPE-19 cells with the widely used autophagosome marker LC3, the mammalian homolog of Atg8. Whereas control cells showed a small number of perinuclear GFP-LC3– or RFP-LC3–positive aggregates, cells treated with CQ for 1 hour began to show ring-shaped AVs that were likely autophagosomes; these increased in number after 6 hours (Fig. 2A). In samples from ARPE-19 cells not transfected with LC3, Western blot analysis with the anti–LC3 antibody showed that LC3-II began to increase 1 hour after treatment with CQ and further increased with time (Fig. 2B). In contrast, the levels of beclin-1, another protein necessary for autophagy, increased at 1 hour but returned to baseline within 6 hours and remained at this level at 12 hours (Fig. 2C)[17]. Then we examined whether protein degradation by autophagy was also activated in CQ-treated cells. We performed immunoblot analysis with the anti–p62 antibody. p62 protein interacts with both LC3-II and ubiquitin protein[18,19] and is degraded in autophagolysosomes. Therefore, a reduction of p62 indicates increased autophagic degradation, whereas an increase of p62 indicates inhibited autophagic degradation.[20] With CQ, the level of p62 signifi-

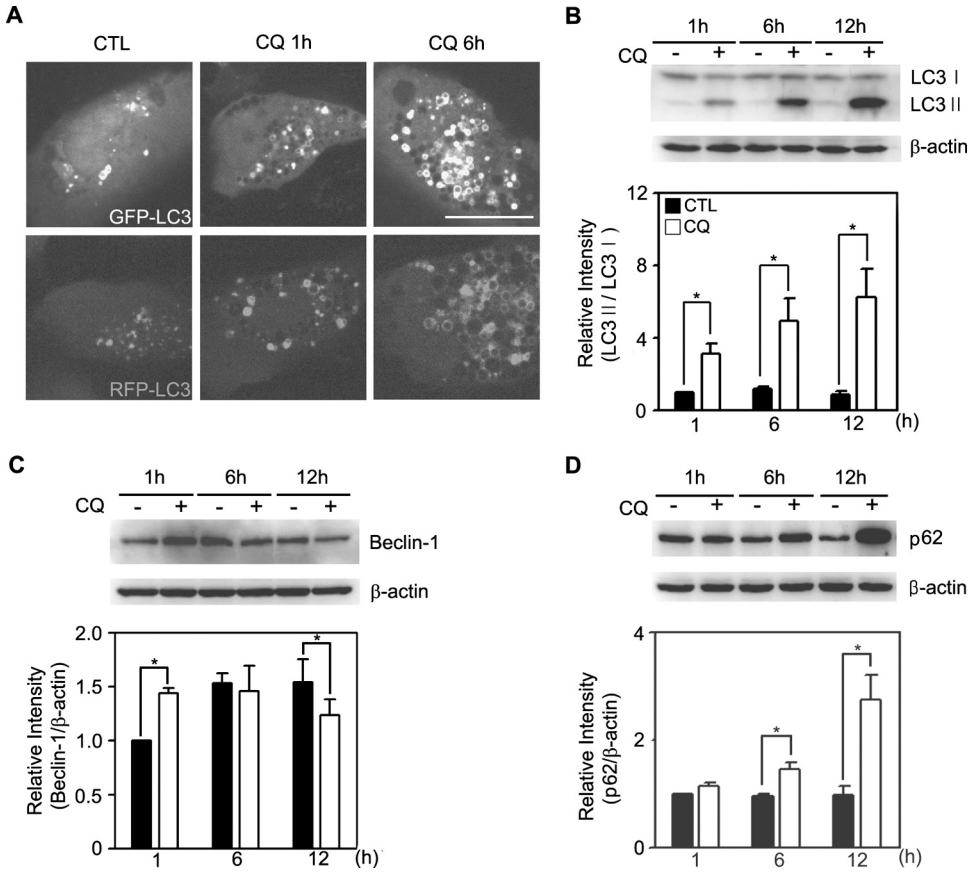

Figure 2. Autophagy markers are increased in CQ-treated ARPE-19 cells. (**A**) Fluorescence microscopic images of GFP-LC3 or RFP-LC3–transfected ARPE-19 cells, sham-washed (CTL) or exposed to 120 μM CQ for 1 hour or 6 hours. Scale bar, 10 μm. Note ring-shaped LC3-positive autophagosomes in CQ-treated cells. (**B**) Samples from sham-washed controls and CQ-treated (120 μM) cells immunoblotted for LC3. Levels of LC3-II, the active form, began to increase at 1 hour and were substantially higher at 6 and 12 hours. Bars denote fold increases in densitometric values of the LC3-II band, normalized to the density of the corresponding LC3-I band and expressed as mean ± SD (*$P < 0.05$; $n = 3$). (**C**) Samples from sham-washed controls and CQ-treated (120 μM) cells immunoblotted for beclin-1. Levels of beclin-1 increased at 1 hour but returned to the baseline at 6 and 12 hours. Bars denote fold increases in densitometric values of the beclin-1 band, normalized to the density of the corresponding actin band and expressed as mean ± SD (*$P < 0.05$; $n = 4$). (**D**) Samples from sham-washed controls and CQ-treated (120 μM) cells immunoblotted for p62. Levels of p62 differed little from control at 1 hour but significantly increased at 6 and 12 hours. Bars denote fold increases in densitometric values of the p62 band, normalized to the density of the corresponding actin band and expressed as mean ± SD (*$P < 0.05$; $n = 4$).

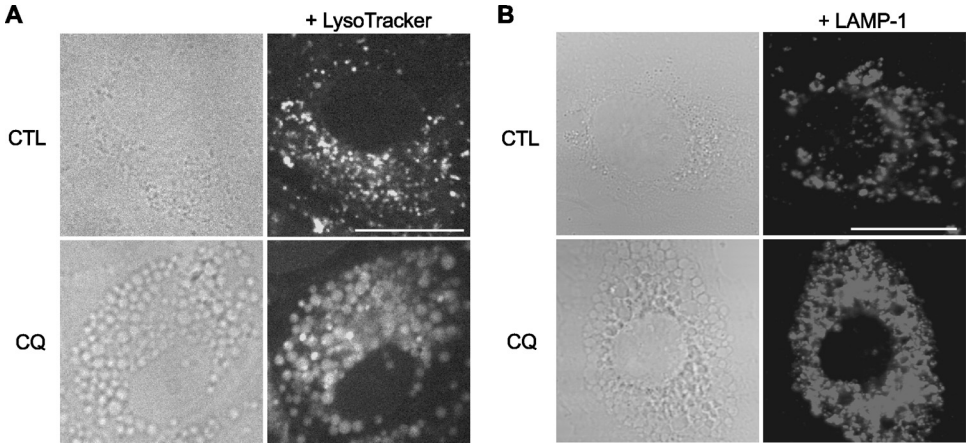

FIGURE 3. CQ treatment induces lysosomal dilatation. (**A**) Bright-field and corresponding solution in dimethyl sulfoxide–stained confocal microscopic images of ARPE-19 cells 2 hours after sham wash (CTL) or after the addition of 120 μM CQ to the medium. Vacuoles formed after CQ treatment corresponded closely to dilated lysosomes. Scale bar, 10 μm. (**B**) Bright-field and corresponding anti–LAMP-1 antibody immunostained confocal microscopic images of ARPE-19 cells, sham-washed controls (CTL), and CQ-treated (120 μM) for 2 hours. Scale bar, 20 μm.

cantly increased 6 to 12 hours after exposure (Fig. 2D), indicating that autophagic degradation was inhibited.

Lysosomal Dilatation by CQ Treatment

Because vacuoles were already formed after 1 hour of CQ treatment (Fig. 1A), when autophagy had just begun to get activated, most vacuoles were likely initially derived from a source other than AVs. To examine the possibility that these vacuoles were derived from specific organelles, we performed live-cell confocal microscopy using a dye for lysosomes (LysoTracker; Invitrogen) and immunostaining with anti–LAMP-1 antibody. Whereas lysosomes were small in control cells, they were greatly dilated in cells treated for 2 hours with CQ and corresponded closely to vacuoles (Figs. 3A, 3B). Our results are in agreement with those of other reports suggesting that the site of toxic actions of CQ is likely lysosomes.[10,21,22] CQ may accumulate preferentially in lysosomes because they are acidic vesicles. If acidity is a prerequisite for CQ accumulation in lysosomes, the inhibition of lysosomal acidification should block the toxic effects of CQ. Consistent with this, the vacuolar H^+-ATPase (V-ATPase) inhibitor bafilomycin A1 completely blocked CQ-induced vacuole formation and cell death in ARPE-19 cells (Fig. 4).

Failure of the Fusion between Autophagosomes and Dilated Lysosomes in CQ-Treated Cells

The final stage of autophagy is the fusion of autophagosomes with lysosomes[23]. To examine this step, we stained RFP-LC3–transfected ARPE-19 cells with solution in dimethyl sulfoxide (LysoTracker Green DND-26; Invitrogen) and observed them with live-cell confocal microscopy. At the same time, we performed double immunostaining with anti–LC3 and anti–LAMP-1 antibodies because the intensity of the dye (LysoTracker Green DND-26; Invitrogen) is changed by pH difference. As a positive control, ARPE-19 cells were treated with 0.5 μM rapamycin for 6 hours, which induced normal autophagy, including fusion between autophagosomes and lysosomes. In rapamycin-treated cells, in which autophagy was expected to be functional, LC3 and lysosomal signals significantly overlapped (Figs. 5A, 5B). In contrast, ARPE-19 cells treated with 120 μM CQ for 2 and 6 hours exhibited almost complete separation between the two signals, indicating that autophagosome-lysosome fusion was severely inhibited (Figs. 5A, 5B).

Accumulation of Ubiquitinated Proteins in Lysosomes of CQ-Treated Cells

The inhibition of autophagy indicates that bulk protein degradation by lysosomes should be impaired. Whereas ubiquitinated proteins are mainly degraded by proteasomes, recent evidence indicates that lysosomal dysfunction causes increases in ubiquitinated proteins.[24] Because accumulation of ubiquitinated proteins may exert cytotoxic effects,[25,26] we examined whether CQ treatment induced increases in the levels of ubiquitinated proteins. As a positive control, we used MG132, an inhibitor of proteasomes, which increased the expression of typical ubiquitinated proteins. Western blot analyses showed that CQ treatment increased the levels of ubiquitinated proteins to an extent similar to those of the proteasome inhibitor MG132 (Fig. 6A). Fluorescence microscopy revealed a particulate pattern of ubiquitin immunoreactivity in CQ- and MG132-treated ARPE cells (Fig. 6B). Of note, there seemed to be differences in the sizes of ubiquitin immunoreactivities. The fact that lysosomes are likely the site of ubiquitinated protein accumulation in CQ, and of proteasome or cytoplasm accumulation in MG132, may explain this difference.

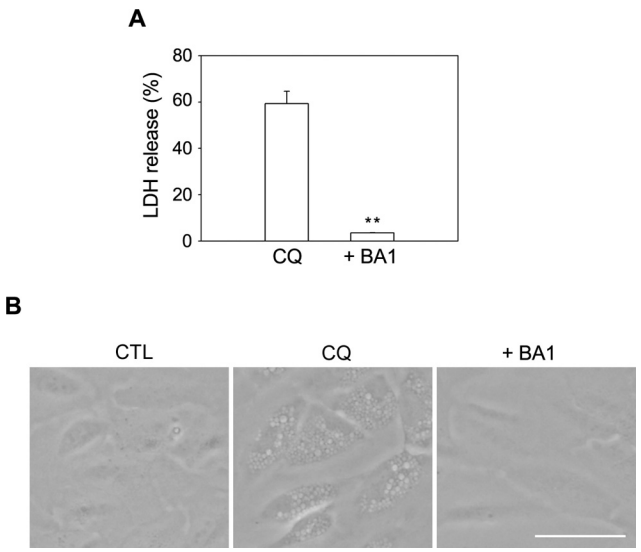

FIGURE 4. Bafilomycin A1 inhibits vacuole formation, lysosomal enzyme dysfunction, and cell death in CQ-treated cells. (**A**) Bars denote LDH release (mean ± SD) by ARPE-19 cells treated with CQ (120 μM, 24 hours) alone or with CQ and 10 nM bafilomycin A1 (BA1). BA1 reduced CQ-induced cell death ($^{**}P < 0.01$, compared with sham-washed controls; $n = 3$). (**B**) Phase-contrast photomicrographs of ARPE-19 cells, sham-washed or treated for 6 hours with 120 μM CQ alone or CQ plus 10 nM BA1. CQ-induced vacuole formation was completely inhibited by BA1. Scale bar, 50 μm.

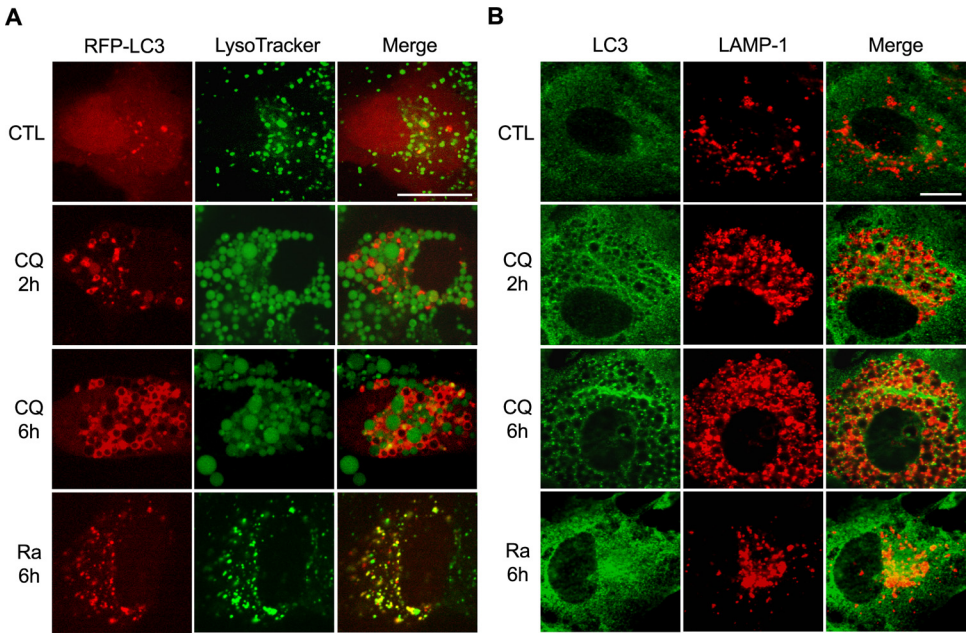

FIGURE 5. Autophagosomes and lysosomes failed to fuse in CQ-treated cells. (**A**) Live-cell confocal microscopic images of RFP-LC3–transfected ARPE-19 cells, sham-washed, treated with 120 μM CQ for 2 or 6 hours, or treated with 0.5 μM rapamycin for 6 hours. Confocal images were taken from a single z-section. Scale bar, 10 μm. (**B**) Double-immunocytochemical staining of ARPE-19 cells with anti–LC3 and anti–LAMP-1 antibodies. Cells were sham washed or treated for 2 or 6 hours with CQ (120 μM) or 0.5 μM rapamycin for 6 hours. Fusion between autophagosomes and lysosomes (*yellow*) was evident in rapamycin-treated cells, but a nearly complete separation between ring-shaped autophagosomes and dilated lysosomes was evident in CQ-treated cells. Scale bar, 10 μm.

We then examined whether ubiquitinated proteins in CQ-treated cells were localized in lysosomes or autophagosomes. In ARPE-19 cells double-immunostained with anti–ubiquitin and anti–LAMP-1 antibodies, both immunoreactivities substantially overlapped (Fig. 7A). In contrast, RFP-LC3–transfected cells stained with an anti–ubiquitin antibody showed little evidence of overlap (Fig. 7B). These data indicate that in CQ-treated ARPE cells, ubiquitinated proteins accumulate mainly in dilated lysosomes.

Increased Accumulation of Exogenously Expressed HttQ74 Aggregates in CQ-Treated Cells

We further examined the functional significance of autophagy inhibition by CQ using the accumulation of exogenously expressed human huntingtin with extended CAG repeat numbers (HttQ74) as a surrogate marker for protein degradation in ARPE-19 cells. In cells transfected with an HttQ74 expression construct, aggregates of GFP-HttQ74 gradually accumulated (arrow) and cell death occurred (Figs. 8A, 8B). In addition, immunoblots showed that the levels of GFP-HttQ74 increased (Figs. 8C, 8D). Hence, CQ seemed to inhibit the clearance of HttQ74, probably because of arrested autophagy/lysosomal function.

Cell Death Mechanism

Although lysosomal accumulation of CQ is required for CQ-induced vacuole formation and cell death (Fig. 4), the downstream death mechanism is unclear. To address this, we first examined whether CQ-induced cell death occurred by so-called autophagic cell death. Although the definition of autophagic cell death is still a matter of some disagreement, the most widely used working criterion is the inhibition of cell death by various inhibitors of autophagy. Using this criterion, autophagic cell death did not seem to be responsible because 3-MA, a potent inhibitor of autophagy, failed to reduce CQ-induced cell death (Fig. 9A). Instead, the inhibition of autophagy with 3-MA significantly potentiated CQ-induced cell death (Fig. 9A), consistent with the interpretation that the blockade of autophagy contributes to cell death. We next examined whether CQ-induced cell death occurred by caspase-dependent apoptosis. Arguing against this possibility, the broad-spectrum caspase inhibitor z-VAD-FMK did not reduce CQ-induced cell death, but staurosporine, an apoptosis inducer, induced cell death (Fig. 9B). Consistent with this, no activation of caspase-3 was detected by Western blot analyses or caspase-3 activity assays (Figs. 9C, 9D). Lastly, we examined whether oxidative stress was the key mechanism of CQ-induced cell death. This was also unlikely because the antioxidants (NAC and Trolox [Hoffman-LaRoch]) failed to reduce cell death. However, H_2O_2-induced cell death was blocked by antioxidants (Fig. 9E). Moreover, there was little increase in DCF fluorescence in CQ-treated cells (Fig. 9F), indicating that ROS levels were largely unchanged. These negative results indicate that CQ-induced cell death may not occur by a single mechanism such as apoptosis, autophagic cell death, or oxidative injury. Instead, CQ-induced cell death may involve the accumulation of ubiquitinated proteins or severe lysosomal dysfunction, such as lysosomal membrane permeabilization.

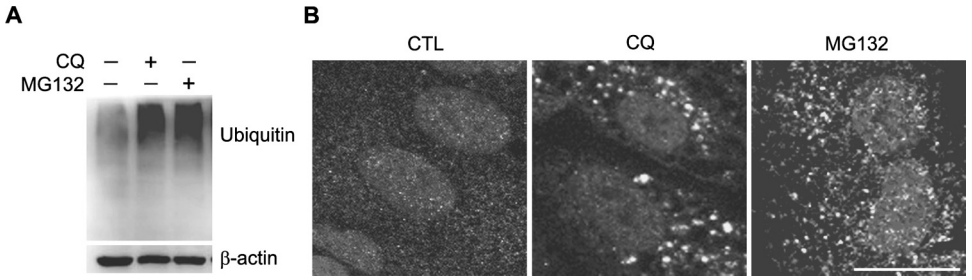

FIGURE 6. Ubiquitinated proteins accumulate in CQ-treated cells. (**A**) Immunoblots for ubiquitinated proteins in samples prepared from sham-washed controls or cells treated for 6 hours with CQ (120 μM) or MG132 (5 μM). (**B**) Immunostaining for ubiquitin in cells treated with CQ or MG132 for 6 hours. Both CQ and MG132 increased the levels of ubiquitinated proteins. Scale bar, 20 μm.

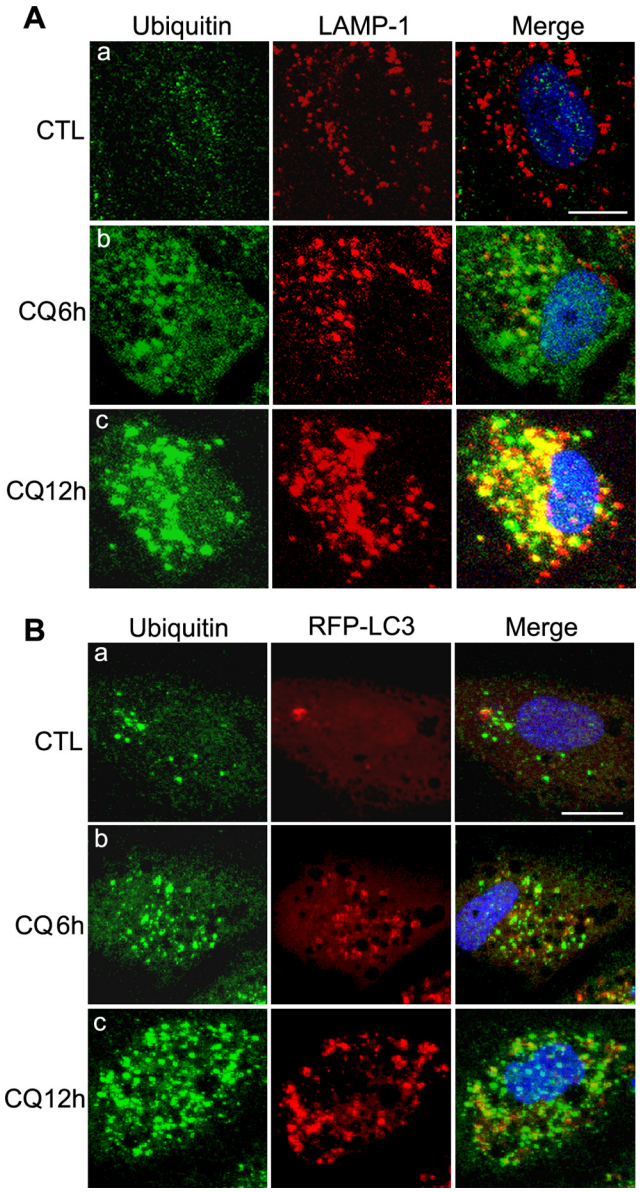

FIGURE 7. Ubiquitinated proteins are colocalized with lysosomes. (**A**) Double-immunocytochemical staining of ARPE-19 cells with anti–LAMP-1 and anti–ubiquitin antibodies. Cells were sham washed or treated for 6 or 12 hours with CQ (120 μM). Whereas ubiquitin immunoreactivity initially appeared mainly outside lysosomes, a substantial fraction of ubiquitin immunostaining later appeared to be associated with LAMP-1 immunoreactivity. Scale bar, 10 μm. (**B**) ARPE-19 cells were transfected with RFP-LC3 plasmids 24 hours before sham wash or before initiation of a 12-hour exposure to 120 μM CQ. After exposure, cultures were fixed and stained with an anti–ubiquitin antibody. Signals for LC3 and ubiquitin overlapped only slightly, indicating that most ubiquitinated proteins did not accumulate in autophagosomes. Scale bar, 10 μm.

DISCUSSION

The incidence of retinopathy associated with CQ treatment reportedly ranges from 0.5% to 1%.[6,27] Although this condition is largely reversible, in a small number of cases it can cause permanent damage such as vision loss associated with bull's eye maculopathy.[28,29] Although the mechanism of CQ-induced retinopathy is not entirely clear, it has been proposed that the inhibition of lysosomal activity may contribute to the ocular side effects of CQ.[30] Given that many cell types exhibit sensitivity to CQ toxicity,[24,31–33] it is puzzling that the RPE is primarily involved in human patients. This may be because of tissue differences in concentration (dose)-dependency or pharmacokinetics (e.g., distribution, clearance). Alternatively, the phagocytosis of the shed outer segment of photoreceptors, a well-known function of RPE, may provide more lysosomal stress to these cells than to other cells. Hence, lysosomal dysfunction may lead to an abnormal accumulation of endocytosed proteins and lipids, which may exert cytotoxic effects on RPE cells.

The results of the present study largely agree with this possibility. In human RPE-derived ARPE-19 cells, the initial morphologic change observed after treatment with CQ was the enlargement of lysosomes, which appear, under a light microscope, as conspicuous cytosolic vacuoles. Although it is unclear how lysosomal enlargement results, it may be that because CQ is a weak base, it accumulates preferentially in acidic compartments such as lysosomes,[34,35] causing local derangements. In support of this supposition, we found that lysosomal acidification was necessary for CQ accumulation in lysosomes, as evidenced by the nearly complete prevention of CQ-induced vacuole formation and cell death by bafilimycin A1, which inhibits lysosomal acidification. One consequence of CQ-induced lysosomal changes is an apparent defect in the fusion of lysosomes with upstream phagosomes, such as autophagosomes and endosomes. Our results clearly demonstrated that autophagosomes remained separate from lysosomes throughout the duration of CQ treatment.

CQ increased the levels of the autophagic markers LC3-II and beclin-1 in ARPE-19 cells. Once autophagy is initiated by the action of ATG7 and ATG3,[36,37] LC3 is converted to the active LC3-II form, which is inserted into the double membrane of autophagophores and autophagosomes. After the fusion of autophagosomes with lysosomes, the LC3-II in the inner membrane is degraded, whereas LC3-II in the outer membrane remains for a time before it is recycled. Another marker, beclin-1, belongs to the class 3 phosphoinositide 3-kinase (PI3K) complex and is involved in the early stages of autophagosome formation.[38,39] It is well known that the inhibition of fusion between autophagosomes and lysosomes causes secondary increases in autophagic markers such as LC3 and beclin-1.[33,40,41] Hence, it is likely that the apparent induction of autophagy by CQ is also a secondary effect of the fusion failure. Consistent with this, CQ treatment resulted in marked increases in the level of lysosome-associated ubiquitinated proteins. Furthermore, the clearance of aggregated mHttp in transfected cells was inhibited by CQ. These findings indicate that abnormalities in autophagy-dependent protein degradation in lysosomes may contribute to CQ-induced retinopathy.

CQ induced not only vacuolar changes but also cell death in the ARPE-19 cell line. Because RPE cells undergo degeneration and cell death in CQ-induced retinopathy,[22,42] understanding the mechanism of cell death may be key to understanding the pathogenesis. Because the levels of some autophagic markers were increased, an autophagic mechanism of cell death might be plausible. However, our demonstration that 3-MA, an inhibitor of the PI3K involved in the early steps of autophagy, failed to attenuate cell death seem to exclude this possibility. In addition, CQ-induced autophagy does not proceed to the level of the lysosomal stage because of this fusion failure. Another mechanism by which CQ might induce cell death is caspase-mediated apoptosis. However, we failed to detect increases in levels of the active form of caspase-3 in CQ-treated cells, and zVAD-FMK did not

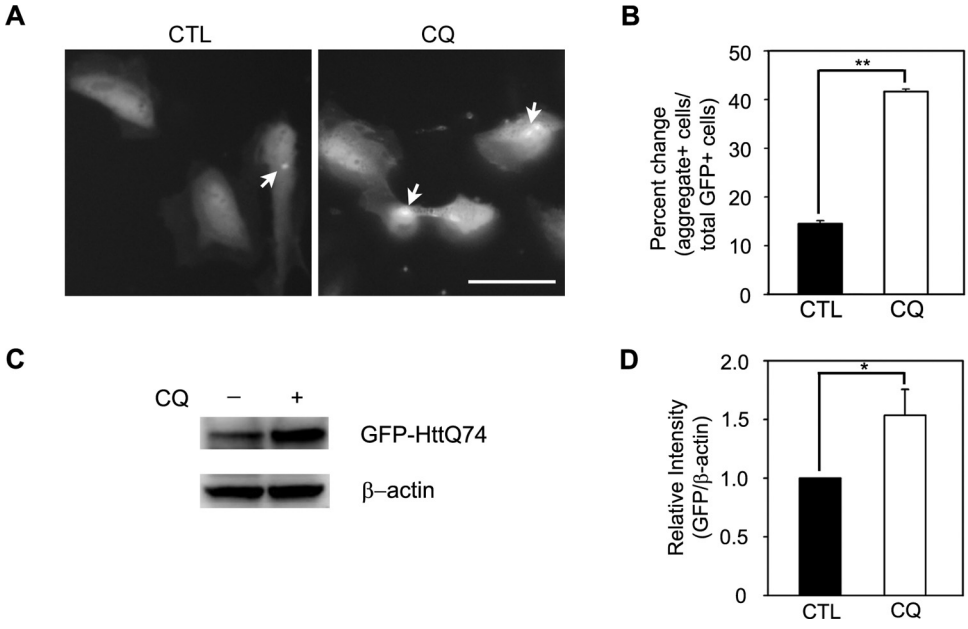

FIGURE 8. CQ delays the clearance of exogenously expressed GFP-HttQ74 in ARPE-19 cells. (**A**) Fluorescence photomicrographs of ARPE-19 cells transfected with a GFP-mHttQ74 expression construct. Compared with sham wash only (CTL), cultures treated for 6 hours with 120 μM CQ exhibited increased amounts of GFP-positive protein aggregates (*arrows*). Scale bar, 50 μm. (**B**) Bars denote the percentage of total GFP-positive cells that contain aggregates in sham-washed controls and cells treated with 120 μM CQ, expressed as mean ± SD ($^{**}P < 0.01$; $n = 3$). (**C**) Immunoblots for GFP-HttQ74. GFP-HttQ74 levels increased in cells treated with 120 μM CQ for 6 hours. (**D**) Bars denote fold increases in densitometric values of the GFP band, normalized to the density of the corresponding actin band and expressed as mean ± SD ($^{*}P < 0.05$; $n = 3$).

attenuate CQ-induced cell death. Hence, it seems unlikely that caspase-mediated apoptosis is the major mechanism underlying CQ-induced RPE cell death. In addition, the antioxidants (NAC and Trolox; Hoffman-LaRoche) failed to reduce cell death induced by CQ. This negative result lessens the possibility that oxidative stress plays a large role in CQ-induced RPE cell death. However, because we used only two kinds of antioxidants, we cannot completely rule out this possibility. Although our results do not precisely define the mechanisms of CQ-induced cell death, we speculate that marked increases in ubiquitinated proteins, which can be cytotoxic through as yet unidentified mechanisms, may play a role in the cytotoxicity of CQ. Additional studies will be needed to confirm this hypothesis.

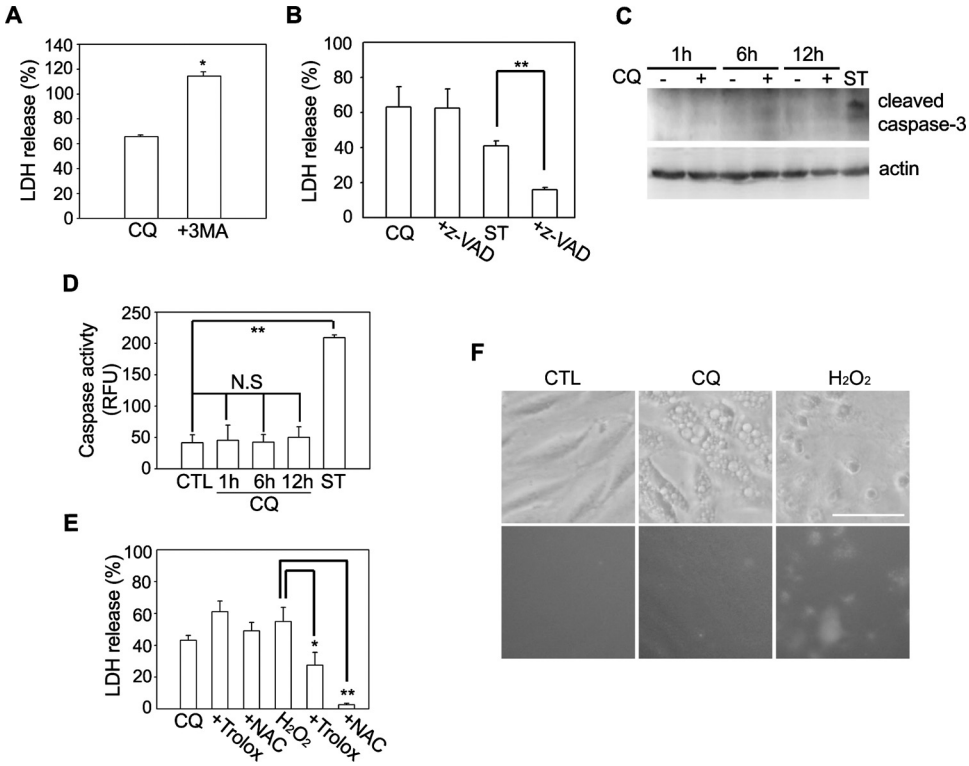

FIGURE 9. Cell death mechanism. (**A**) Bars denote LDH release (mean ± SD) in ARPE-19 cells treated with CQ (120 μM, 24 hours), alone or with CQ and 2.5 mM 3-MA. 3-MA potentiated CQ-induced cell death ($^{*}P < 0.05$, compared with sham-washed controls; $n = 3$). (**B**) Bars represent LDH release in cells treated with CQ alone (120 μM, 24 hours) or with CQ and 50 μM z-VAD-FMK or with staurosporine (ST) alone (1 μM, 24 hours) or with ST and z-VAD-FMK, respectively. The z-VAD FMK did not protect against CQ-induced cell death, whereas it did inhibit ST-induced cell death ($^{**}P < 0.01$, compared with ST alone; $n = 3$). (**C**) Western blot analysis for cleaved (active) casapase-3. No increase in the level of active caspase-3 was seen in CQ-treated cells. In contrast, a 12-hour exposure to 100 nM ST increased active caspase-3 levels. (**D**) Bars indicate caspase activity in control ARPE-19 cell cultures and cells treated with 120 μM CQ for 1 hour to 12 hours. Data represent the relative fluorescence units (RFUs) per million cells expressed as mean ± SD. No increase in caspase activity was seen. In contrast, caspase activity was greatly increased in cultures exposed to 100 nM ST for 12 hours ($^{**}P < 0.01$, compared with sham-washed controls; $n = 3$). N.S., not significant. (**E**) LDH release (mean ± SEM, $n = 3$) in cells treated with CQ (120 μM, 24 hours) alone, H_2O_2 alone (150 μM, 24 hours), or in combination with 1 mM NAC or 0.1 mM antioxidant. H_2O_2-induced cell death was inhibited by antioxidants, but CQ-induced cell death was not attenuated by antioxidants ($^{*}P < 0.05$ and $^{**}P < 0.01$, compared with H_2O_2 alone; $n = 3$). (**F**) Fluorescence photomicrographs of ARPE-19 cells stained with H_2-DCFDA. Whereas DCF fluorescence increased 12 hours after exposure to 500 μM H_2O_2, there was no such increase in fluorescence 12 hours after the onset of CQ exposure. Scale bar, 50 μm.

The present study has demonstrated several features of CQ-induced cytotoxicity in ARPE-19 cells, namely enlarged lysosomes (vacuolar changes), failure of fusion between AVs and lysosomes, secondary increases in the levels of autophagy markers, and cell death. Although it is unclear which of these changes is most relevant in human CQ-induced retinopathy, the present results may provide insights to guide the development of protective measures.

References

1. Freedman A. Chloroquine and rheumatoid arthritis: a short-term controlled trial. *Ann Rheum Dis.* 1956;15:251–257.
2. Mackenzie AH. Antimalarial drugs for rheumatoid arthritis. *Am J Med.* 1983;75:48–58.
3. Rynes RI. Antimalarial drugs in the treatment of rheumatological diseases. *Br J Rheumatol.* 1997;36:799–805.
4. Hamano T, Gendron TF, Causevic E, et al. Autophagic-lysosomal perturbation enhances tau aggregation in transfectants with induced wild-type tau expression. *Eur J Neurosci.* 2008;27:1119–1130.
5. Rosenthal AR, Kolb H, Bergsma D, Huxsoll D, Hopkins JL. Chloroquine retinopathy in the rhesus monkey. *Invest Ophthalmol Vis Sci.* 1978;17:1158–1175.
6. Tehrani R, Ostrowski RA, Hariman R, Jay WM. Ocular toxicity of hydroxychloroquine. *Semin Ophthalmol.* 2008;23:201–209.
7. Gaynes BI, Torczynski E, Varro Z, Grostern R, Perlman J. Retinal toxicity of chloroquine hydrochloride administered by intraperitoneal injection. *J Appl Toxicol.* 2008;28:895–900.
8. Maenpaa H, Toimela T, Mannerstrom M, Saransaari P, Tahti H. Toxicity of selected cationic drugs in retinoblastomal cultures and in cocultures of retinoblastomal and retinal pigment epithelial cell lines. *Neurochem Res.* 2004;29:305–311.
9. Peters S, Reinthal E, Blitgen-Heinecke P, Bartz-Schmidt KU, Schraermeyer U. Inhibition of lysosomal degradation in retinal pigment epithelium cells induces exocytosis of phagocytic residual material at the basolateral plasma membrane. *Ophthalmic Res.* 2006;38:83–88.
10. Sundelin SP, Terman A. Different effects of chloroquine and hydroxychloroquine on lysosomal function in cultured retinal pigment epithelial cells. *APMIS.* 2002;110:481–489.
11. Wetterholm DH, Winter FC. Histopathology of chloroquine retinal toxicity. *Arch Ophthalmol.* 1964;71:82–87.
12. Bok D. Retinal photoreceptor-pigment epithelium interactions: Friedenwald lecture. *Invest Ophthalmol Vis Sci.* 1985;26:1659–1694.
13. Bosch E, Horwitz J, Bok D. Phagocytosis of outer segments by retinal pigment epithelium: phagosome-lysosome interaction. *J Histochem Cytochem.* 1993;41:253–263.
14. Kelekar A. Autophagy. *Ann N Y Acad Sci.* 2005;1066:259–271.
15. Tanida I, Ueno T, Kominami E. LC3 conjugation system in mammalian autophagy. *Int J Biochem Cell Biol.* 2004;36:2503–2518.
16. Koh JY, Choi DW. Quantitative determination of glutamate mediated cortical neuronal injury in cell culture by lactate dehydrogenase efflux assay. *J Neurosci Methods.* 1987;20:83–90.
17. Yang C, Kaushal V, Shah SV, Kaushal GP. Autophagy is associated with apoptosis in cisplatin injury to renal tubular epithelial cells. *Am J Physiol Renal Physiol.* 2008;294:F777–F787.
18. Bauvy C, Meijer AJ, Codogno P. Assaying of autophagic protein degradation. *Methods Enzymol.* 2009;452:47–61.
19. Mizushima N, Yoshimori T. How to interpret LC3 immunoblotting. *Autophagy.* 2007;3:542–545.
20. Bjorkoy G, Lamark T, Pankiv S, Overvatn A, Brech A, Johansen T. Monitoring autophagic degradation of p62/SQSTM1. *Methods Enzymol.* 2009;452:181–197.
21. Butler D, Brown QB, Chin DJ, et al. Cellular responses to protein accumulation involve autophagy and lysosomal enzyme activation. *Rejuvenation Res.* 2005;8:227–237.
22. Mahon GJ, Anderson HR, Gardiner TA, McFarlane S, Archer DB, Stitt AW. Chloroquine causes lysosomal dysfunction in neural retina and RPE: implications for retinopathy. *Curr Eye Res.* 2004;28:277–284.
23. Bains M, Heidenreich KA. Live-cell imaging of autophagy induction and autophagosome-lysosome fusion in primary cultured neurons. *Methods Enzymol.* 2009;453:145–158.
24. Carew JS, Medina EC, Esquivel JA 2nd, et al. Autophagy inhibition enhances vorinostat-induced apoptosis via ubiquitinated protein accumulation. *J Cell Mol Med.* In press.
25. Canu N, Barbato C, Ciotti MT, Serafino A, Dus L, Calissano P. Proteasome involvement and accumulation of ubiquitinated proteins in cerebellar granule neurons undergoing apoptosis. *J Neurosci.* 2000;20:589–599.
26. Li Z, Jansen M, Pierre SR, Figueiredo-Pereira ME. Neurodegeneration: linking ubiquitin/proteasome pathway impairment with inflammation. *Int J Biochem Cell Biol.* 2003;35:547–552.
27. Yam JC, Kwok AK. Ocular toxicity of hydroxychloroquine. *Hong Kong Med J.* 2006;12:294–304.
28. Shinjo SK, Maia OO Jr, Tizziani VA, et al. Chloroquine-induced bull's eye maculopathy in rheumatoid arthritis: related to disease duration? *Clin Rheumatol.* 2007;26:1248–1253.
29. Tanenbaum L, Tuffanelli DL. Antimalarial agents: chloroquine, hydroxychloroquine, and quinacrine. *Arch Dermatol.* 1980;116:587–591.
30. Liu J, Lu W, Reigada D, Nguyen J, Laties AM, Mitchell CH. Restoration of lysosomal pH in RPE cells from cultured human and ABCA4(−/−) mice: pharmacologic approaches and functional recovery. *Invest Ophthalmol Vis Sci.* 2008;49:772–780.
31. Boya P, Gonzalez-Polo RA, Casares N, et al. Inhibition of macroautophagy triggers apoptosis. *Mol Cell Biol.* 2005;25:1025–1040.
32. Iwai-Kanai E, Yuan H, Huang C, et al. A method to measure cardiac autophagic flux in vivo. *Autophagy.* 2008;4:322–329.
33. Shacka JJ, Klocke BJ, Shibata M, et al. Bafilomycin A1 inhibits chloroquine-induced death of cerebellar granule neurons. *Mol Pharmacol.* 2006;69:1125–1136.
34. Namazi MR. The potential negative impact of proton pump inhibitors on the immunopharmacologic effects of chloroquine and hydroxychloroquine. *Lupus.* 2009;18:104–105.
35. Poole B, Ohkuma S. Effect of weak bases on the intralysosomal pH in mouse peritoneal macrophages. *J Cell Biol.* 1981;90:665–669.
36. Eskelinen EL. New insights into the mechanisms of macroautophagy in mammalian cells. *Int Rev Cell Mol Biol.* 2008;266:207–247.
37. Maiuri MC, Zalckvar E, Kimchi A, Kroemer G. Self-eating and self-killing: crosstalk between autophagy and apoptosis. *Nat Rev Mol Cell Biol.* 2007;8:741–752.
38. Ferraro E, Cecconi F. Autophagic and apoptotic response to stress signals in mammalian cells. *Arch Biochem Biophys.* 2007;462:210–219.
39. Sinha S, Levine B. The autophagy effector Beclin 1: a novel BH3-only protein. *Oncogene.* 2008;27(suppl 1):S137–S148.
40. Wu YC, Wu WK, Li Y, et al. Inhibition of macroautophagy by bafilomycin A1 lowers proliferation and induces apoptosis in colon cancer cells. *Biochem Biophys Res Commun.* 2009;382:451–456.
41. Ramser B, Kokot A, Metze D, Weiss N, Luger TA, Bohm M. Hydroxychloroquine modulates metabolic activity and proliferation and induces autophagic cell death of human dermal fibroblasts. *J Invest Dermatol.* 2009;129:2419–2426.
42. Kellner U, Kellner S, Weinitz S. Chloroquine retinopathy: lipofuscin- and melanin-related fundus autofluorescence, optical coherence tomography and multifocal electroretinography. *Doc Ophthalmol.* 2008;116:119–127.